77-010. Southwestern Research Institute, San Antonio, Texas, July 1977.
19. C.M. Urban. Heavy-Duty Fuel Economy Program: Phase III, Transient Cycle Evaluations of the Advanced Emissions Control Technology Engineer. EPA-460/3/78-005. Southwestern Research Institute, San Antonio, Texas, May 1978.
20. Federal Register, Vol. 42, No. 174, Sept. 8, 1977.
21. F.T. Buckley, Jr., C.H. Marks, and H.W. Walston, Jr. Analysis of Coast-Down Data to Access Aerodynamic Drag Reduction on Full-Scale Tractor-Trailer Trucks in Windy Environments. Report 760850. Society of Automotive Engineers Transactions, Mechanical Engineering Department, University of Maryland, College Park, 1976.
22. F.-P. Lee, C.E. Lee, R.B. Machemehl, and C.R. Copeland, Jr. Vehicle Emissions at Intersections. Research Report 250-1. Center for Transportation Research, Bureau of Engineering Research, University of Texas at Austin, Aug. 1983.

Publication of this paper sponsored by Committee on Traffic Flow Theory and Characteristics.

Discontinuity in Equilibrium Freeway Traffic Flow

HAROLD J. PAYNE

ABSTRACT

Analysis of freeway traffic flow data reveals a discontinuity in the equilibrium relationship between speed and density, supporting the dual-mode or two-regime theories of traffic flow. This work was done during the development of an appropriate equilibrium speed-density relationship for a dynamic macroscopic freeway simulation model, FREFLO. This context assisted in clarifying the distinction between equilibrium and nonequilibrium conditions in traffic data and as a consequence made the discontinuity in equilibrium conditions perfectly evident. Use of the new relationship greatly improved the quality of FREFLO model predictions. The corresponding discontinuity in the volume that can be maintained appears to have great significance for the design of freeway control systems.

Traffic speeds bear a generally consistent relationship to traffic density (i.e., mean spacing). A multitude of theories has been developed to represent both static, average relationships at a macroscopic level and dynamic relationships at both microscopic and macroscopic levels. These theories are connected by the fact that the possible steady-state conditions of the dynamic models, expressed as a set of speed-density pairs, can be viewed as a macroscopic, equilibrium speed-density relationship.

The earliest work proposed fairly simple speed-density relationships (e.g., speed linearly decreasing with increasing density). However, Edie (1) first observed a difference in character between two regimes of traffic, roughly characterized as uncongested and congested, and proposed a more sophisticated two-regime model for the speed-density relationship. Empirical analyses (2-5) tended to support this view and others investigated this concept (6).

Further support for the existence of two modes of behavior, and in particular for a discontinuity in the speed-density relationship, is provided. This work was done during the development of an appropriate equilibrium speed-density relationship for a dynamic macroscopic freeway simulation model, FREFLO (7,8). This context assisted in clarifying the distinction between equilibrium and nonequilibrium conditions in traffic data and as a consequence made the discontinuity in equilibrium conditions perfectly evident. Use of the new relationship greatly improved the quality of FREFLO model predictions.

This discontinuity also reveals itself as a discontinuity in the volume-density relationship. In this form, implications for freeway control are evident. This was first recognized by Bullen (9), and was elaborated by him and his colleagues (10,11).

The remainder of this paper is organized as follows. The next section describes FREFLO and the role of the equilibrium speed-density relationship in it. Subsequent sections describe the acquisition, preparation, and selection of data; data analysis procedures; and regression results. The final section addresses implications for freeway control.

FREFLO

The TRAFLO simulation code, recently completed under FHWA sponsorship, consists of three street network component models and a macroscopic freeway component model, TRAFLO. FREFLO is the macroscopic freeway component of the TRAFLO simulation code (12). FREFLO, as described in several reports and papers (12-14), is based on an aggregate variable model first developed for simulation purposes by Payne (7).

FREFLO is based on a representation of traffic flow in terms of three aggregate variables:

ρ: traffic density (units: vehicles/lane-mile),
u: (space-mean) speed (units: miles/hour), and
q: volume (units: vehicles/lane-hour).

The freeway itself is represented by a network of freeway sections. Traffic flow is assumed to be homogeneous within a section. The two aggregate variables, ρ and u, describe conditions over a section at an instant in time. Volume, on the other hand, describes the rate of movement of vehicles past section boundaries.

To make FREFLO specific to a site, traffic demand data, geometric data, and traffic flow behavior data must be specified. The traffic flow behavior parameters were the object of the calibration effort described elsewhere (15).

The parameters calibrated were

1. Speed-density relationship parameters, including nominal capacity for each section of roadway, free-flow speed, and several more coefficients that define the shape of the speed-density relationship and
2. Dynamic interaction parameters, including the reaction time coefficient k_T and the anticipation coefficient k_ν.

Attention is restricted to the speed-density relationship. Results pertinent to the dynamic interaction parameters are available elsewhere (15). Freeway traffic surveillance data gathered from the freeway systems in Los Angeles (16,17) were acquired for use in this study.

ACQUISITION, PREPARATION, AND SELECTION OF DATA

Automated surveillance equipment for acquiring speed-density data is available in the Los Angeles area. Occupancy and counts over 20-, 30-, or 60-sec intervals are generated. Speed traps were not in place, so direct measurement of individual speeds was not provided.

With automated surveillance data, the occupancy data can be scaled to obtain density. The appropriate scale factor depends on the traffic mix (distribution of vehicle lengths), the size of the presence detector loop, and the selection of thresholds in the associated electronics. Hence, the appropriate scale factor will be site specific and can vary significantly from one location to another.

Counts yield volume measurements by application of the appropriate factor. For example, 60-sec counts yield hourly volumes according to

Hourly volume = 60 x (60-sec count).

Finally, given any two of the three (desired) measurements, density, speed and volumes, the third can be derived via the relationship

Volume = speed x density.

In Table 1, surveillance data, occupancy, and speed (derived from volume and occupancy) measurements from the Santa Monica Freeway in Los Angeles are given. (Density values were computed from occupancy by applying the scale factor 2.72, a value appropriate for the Los Angeles freeways from which data were obtained for this research.) As suggested in Table 1, attention is focused on station 18.

The dynamic speed-density relationship includes the equilibrium speed-density relationship. It also includes additional terms that are intended to entirely account for spatial and temporal variations in traffic conditions of the FREFLO model (15). To obtain data suitable for calibrating the speed-density relationship, it is necessary to exclude data at times and places where substantial spatial and temporal variations exist. Therefore, in examining data pertaining to a particular location (i.e., a surveillance station) it is necessary to consider data from adjacent stations to properly identify equilibrium data.

Data at a particular station are not suitable if values (of density or speed) at adjacent stations are substantially different, indicative of substantial spatial variations. It is also necessary to observe variations over time within a station; data values are not suitable if adjacent values (in time) are substantially different, indicative of substantial temporal variations.

In Table 1, three segments of data pertaining to station 18 have been distinguished. The first segment contains high-speed, low-density, equilibrium data. The second segment involves nonequilibrium data, so judged because the substantial spatial variations in speed, or occupancy, or both; these data are not used for calibration. The third segment involves low-speed, high-density equilibrium data. Such data will entail some temporal and spatial variations, but there is no persistent difference, as there is in the second segment.

Analysis of Equilibrium Speed-Density Data

The analysis of speed-density data to produce the desired equilibrium speed-density relationship involved two major steps: (a) careful selection of equilibrium data and (b) application of regression software to extract coefficients and measures of fit.

Data Selection

Selection of data for developing the equilibrium speed-density relationship requires great care. Figures 1 through 4 show the differences in the data that arise depending on the degree of care that is taken in selecting data. Figure 1 shows composite data from several adjacent stations on the Santa Monica Freeway. Table 1 gives a portion of that data. It will be observed that there appears to be a continuous reduction of speed with density. However,

TABLE 1 Occupancy and Speed Data from the Santa Monica Freeway in Los Angeles

	OCCUPANCY (%) STATION NUMBER							SPEED (MI/HR) STATION NUMBER							
TIME	15	16	17	18	19	20	21	15	16	17	18	19	20	21	
↓	14	13	13	12	14	14	10	49	53	49	47	44	44	49	HIGH SPEED, LOW
	14	13	12	15	17	14	14	50	54	48	44	45	43	46	DENSITY EQUILIBRIUM
	14	15	14	13	18	18	15	47	50	51	36	41	44	44	DATA
	11	12	15	16	17	18	14	46	49	46	37	40	41	47	
	15	11	10	20	18	15	16	49	50	44	40	39	42	46	
	17	17	15	14	18	19	15	49	53	47	31	40	39	45	
	13	14	18	16	17	16	15	49	52	47	26	41	40	44	
	15	13	14	21	16	17	15	48	53	50	24	40	42	44	
	14	13	15	23	17	19	15	50	51	44	28	40	43	46	NONEQUILIBRIUM DATA:
	14	13	13	25	16	16	16	48	53	40	27	39	41	46	SUBSTANTIAL SPATIAL
	13	12	15	21	16	14	14	44	50	23	20	40	38	46	AND/OR TEMPORAL
	16	14	13	24	19	17	13	42	49	22	22	39	38	42	VARIATIONS IN
	18	14	27	28	18	19	15	43	40	20	21	40	39	42	OCCUPANCY AND/OR
	17	14	25	27	16	17	18	46	24	21	21	38	38	44	SPEED ARE PRESENT
	17	18	29	28	17	16	14	45	21	9	24	40	38	43	
	18	28	32	29	16	17	16	34	28	19	24	36	41	45	
	18	32	49	25	17	18	16	30	15	22	22	37	39	44	
	21	26	31	24	18	14	15	33	13	23	22	37	38	44	
	24	33	30	27	17	17	15	14	21	19	24	32	38	43	
	22	36	26	31	18	20	15	20	27	21	21	37	34	44	
	38	29	31	26	23	18	16	32	19	18	24	37	38	43	
	29	24	28	26	17	21	15	17	21	17	25	35	38	41	
	22	30	30	26	19	19	16	22	21	12	24	34	37	41	
	35	29	32	24	19	18	18	28	20	20	22	36	34	36	
	28	28	42	27	20	16	16	26	8	23	24	34	33	32	
	24	27	28	27	19	20	17	16	16	22	22	37	35	31	
	28	47	27	25	20	23	22	14	24	21	24	37	32	15	
	36	38	28	26	17	20	22	23	28	19	24	35	31	28	
	35	27	30	25	19	20	36	29	28	8	25	36	12	30	
	25	22	35	26	18	23	22	32	26	19	24	32	20	32	
	22	24	51	24	20	40	21	33	16	15	26	26	24	35	
	22	24	32	24	18	32	21	35	18	16	26	16	27	32	LOW SPEED, HIGH
	21	31	35	23	25	26	20	25	23	19	26	21	29	24	DENSITY EQUILIBRIUM
	20	31	32	23	35	24	20	28	12	17	21	18	31	29	DATA
	29	26	33	24	31	23	26	31	15	21	18	15	25	21	
	25	39	34	28	33	21	22	28	20	19	18	16	32	19	

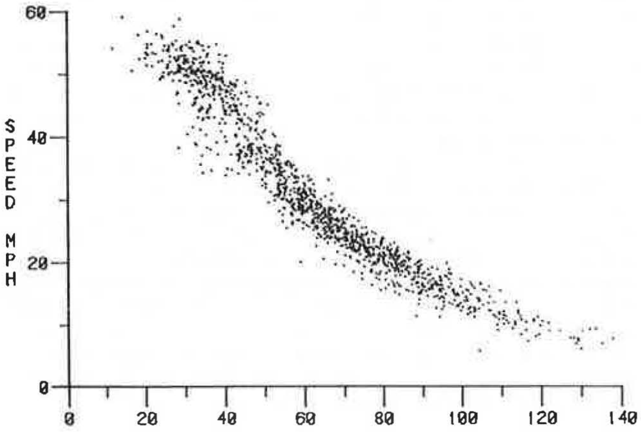

FIGURE 1 Composite scatterplot for several Santa Monica Expressway stations.

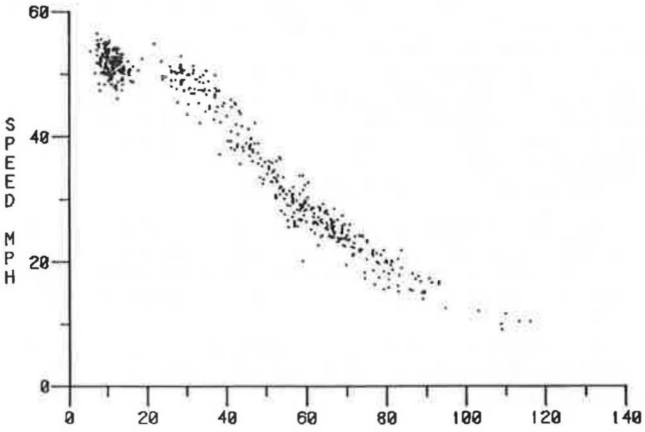

FIGURE 2 Scatterplot for Santa Monica Expressway station 18.

one must recognize that data from different stations involve different electronics so that different scale factors may be required to accurately estimate density from occupancy at the several stations. In the composite data displayed, a single scale factor was applied. In addition, differences in that data for distinct stations can be expected because of local geometrics and resultant differences in traffic behavior. Finally, the data of Figure 1 include data in nonequilibrium conditions.

Figure 2 shows data pertinent to a single station, SME 18. (A portion, but not all, of the data in Figure 2 is present in Figure 1.) Compared with the data in Figure 1, there is clearly a great deal less scatter. These data, however, also contain data in nonequilibrium conditions. Figures 3 and 4 clearly show the distinctive differences among several traffic regimes. In Figure 3, only nonequilibrium data are shown. It will be noted that speeds are generally in the 30- to 40-mph range, with densities in the 40- to 60-vehicles per lane-mile range. Equilibrium data are shown in Figure 4. These data clearly fall into two regimes, corresponding to high-speed flow and congested flow. Most striking, however, is the clear discontinuity in speeds: Equilibrium speeds in the 30- to 40-mph range are rare. Thus, the appearance of continuity of speed as a function of density is seen to be derived from mixing nonequilibrium data with equilibrium data.

In the analyses that were undertaken, data were

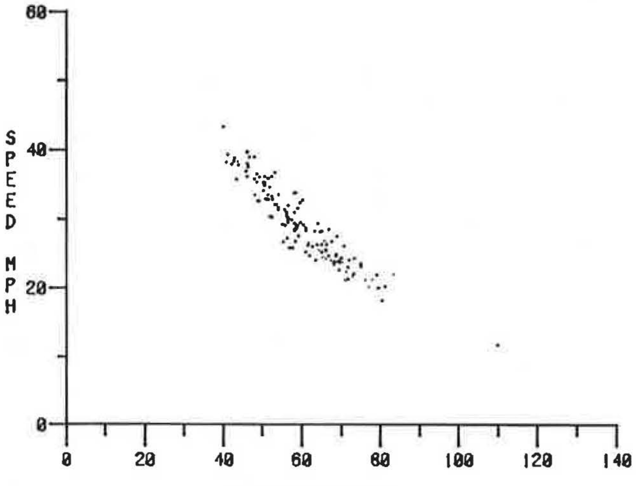

FIGURE 3 Nonequilibrium data for Santa Monica Expressway station 18.

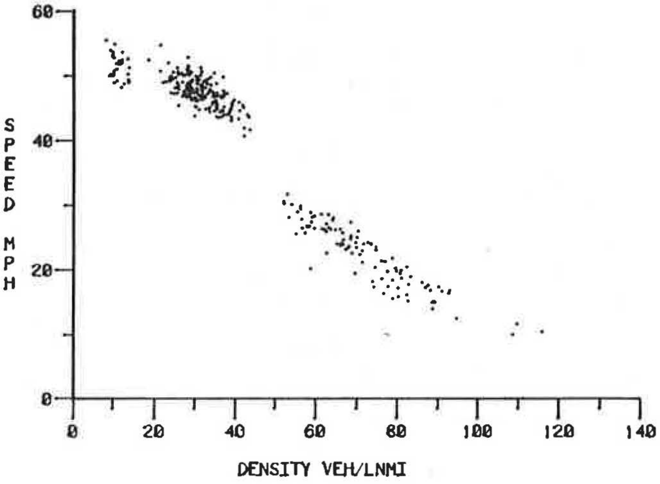

FIGURE 4 Equilibrium data for Santa Monica Expressway station 18.

carefully selected to remove nonequilibrium data. Analyses were first conducted on data from a single station. When a proper understanding of the form of the speed-density relationship was obtained, analysis of a composite data set, formed by aggregating all the station-specific data, was conducted to establish a universal form for the speed-density relationship. The data selected for analysis are given in Table 2.

DATA ANALYSIS PROCEDURES

The steps adopted for determination of the equilibrium speed-density relationship were

1. Selection of data,
2. Selection of functional form,
3. Selection of density breakpoints to define flow regimes,
4. Application of regression technique in each flow regime, and
5. Qualitative and quantitative assessment of alternatives.

TABLE 2 Data Selected for Equilibrium Speed-Density Analysis

STATION	TOTAL NUMBER OF EQUILIBRIUM DATA PAIRS	DATA SET*	NUMBER OF POINTS
SME12	491	740904-62	141
		740904-63	175
		740423-53	175
SME18	301	740904-62	110
		740904-63	30
		740423-53	61
		740423-56	100
HAS13	404	740904-60	130
		740322-01	64
		740325-02	72
		740426-05	138
HAS18	429	740904-60	155
		740322-01	95
		740325-02	88
		740426-05	91
HAS24	170	740904-60	22
		740325-02	88
		740426-05	60

*See Payne *(16)*.

This procedure is of course iterative. Selection of data required careful attention to temporal and spatial variation, as discussed previously.

Functional Forms

Several functional forms were examined, including the two-regime polynomial and inverse polynomial forms and the three-regime forms. The first two functional forms involve one density breakpoint that divides the free-flow from the impeded and constrained flow regime. The third functional form also involves a second density breakpoint, dividing the impeded and constrained flow regimes.

These functional forms were selected by visual inspection of data to select data that provide adequate conformance to the trends and degrees of freedom in matching the data. Data in each regime were treated separately and manipulated as necessary so that linear regression techniques could be applied. Finally, assessment of the alternative results was made to arrive at a standard form for the equilibrium speed-density relationship that is believed appropriate for implementation of FREFLO. The three-regime form is shown in Figure 5.

The method adopted for estimating coefficients from data was to apply linear regression to the data in each of the two- or three-flow regimes separately. In certain circumstances, this required a preliminary manipulation of the data so that a linear regression technique could be applied.

In all instances, the free-flow regime was represented by a constant free-flow speed. The value of free-flow speed was simply obtained as the average of speed values where the corresponding density was below the density breakpoint, ρ_1, defining the free-flow regime.

Three functional forms were considered for the impeded and constrained flow regime:

1. Polynomial,
2. Inverse polynomial, and
3. Shifted inverse polynomial.

The polynomial form,

$$u_e(\rho) = \alpha_0 + \alpha_1 \rho + \alpha_2 \rho^2 + \ldots + \alpha_n \rho^n$$

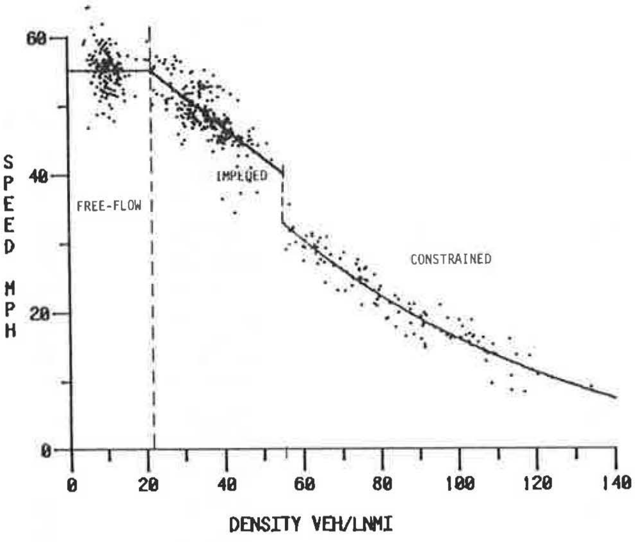

FIGURE 5 Three-regime, discontinuous speed-density relationship.

can be directly treated by standard linear regression techniques. IBM's Scientific Subroutine Package was in fact used for this purpose. The inverse polynomial form

$$u_e(\rho) = 1/(\beta_0 + \beta_1\rho + \beta_2\rho^2 + \ldots + \beta_n\rho^n)$$

can be rewritten as

$$1/u_e(\rho) = \beta_0 + \beta_1\rho + \beta_2\rho^2 + \ldots + \beta_n\rho^n$$

Hence, if each data pair (ρ,u) is replaced by $(\rho,1/u)$, the same standard linear regression technique can be applied. The third form, the shifted inverse polynomial,

$$u_e(\rho) = -u_0 + 1/(\beta_0+\beta_1\rho + \beta_2\rho^2 + \ldots + \beta_n\rho^n)$$

can similarly be written as

$$1/[u_0 + u_e(\rho)] = \beta_0 + \beta_1\rho + \beta_2\rho^2 + \ldots + \beta_n\rho^n$$

so that the data transformation form (ρu) to $[\rho,1/(u_0+u)]$ again allows application of the same technique.

Note that the selection of the density breakpoints and the speed offset (u_0) are not a part of the linear regression technique and must be done before curve fitting. The method adopted was to

1. Select density breakpoints (and speed offset, u_0, in the third form),
2. Apply linear regression in each regime, and
3. Combine results (compute total sum of squared deviations).

Variations in density breakpoints, functional form, polynomial order, and speed offsets produced alternative results that were then assessed quantitatively, using the total sum of squared deviations, and qualitatively, considering the resultant volume-density relationship and the consistency of the selection of breakpoint with actual match of separate regression at the density breakpoint. This method is suboptimal in the sense that an optimal, nonlinear regression technique embodying selection of polynomial coefficients, density breakpoints, and speed offset could have been defined. This method was selected primarily because of its simplicity and economy, which depend on available subroutines.

REGRESSION RESULTS

The methods described earlier were applied to the data sets given in Table 2--initially to each station-specific data set and then to the composite data set. Initial analysis focused on the determination of an appropriate functional form. This effort resulted in selection of the three-regime, discontinuous form. More specifically, it was found that the first-order polynomial form in the impeded regime and the inverse first-order polynomial form in the congested regime were satisfactory.

Results of the regression analysis are given in Table 3. Shown are full calibration results and results for calibration to the standard form. The former is discussed first. Each station-specific data set was subjected to a series of regression analyses, with the functional form fixed as indicated and with variations in density breakpoints and speed offset. Table 3 gives results of these analyses in the form of regression coefficients, selected breakpoints, capacity, and fit. The relative consistency of these results suggested that a universal form might be obtained from the composite data set. Results of that analysis are also given in Table 3.

The results obtained from this analysis of the composite data defined the standard form for the speed-density relationship. This relationship and the corresponding volume-density relationship are shown in Figures 6 and 7, respectively.

The next set of analyses involved application of a second calibration method (15) to each of the station-specific data sets. Each such analysis established a free-flow speed and a scale factor that determined the nominal capacity. The method of arriving at the two parameters was twofold: (a) linear regression to establish free-flow speed and (b) an iterative, mean-square error technique to establish the scale factor. Details appear elsewhere (15). These results are given in Table 3 under the heading "Calibration to Standard Form." The free-flow speed is the same as obtained in the full calibrations. Fits were generally only slightly degraded from the full calibration results.

It is interesting to note that these results imply a corresponding discontinuity in volume at the second breakpoint of significant size. For the standard relationship identified, volume decreased from 2,136 to 1,723 veh/lane-hr at the breakpoint value of 55 veh/lane-mile.

IMPLICATIONS FOR CONTROL

Bullen (9) first called attention to the importance of the dual-mode behavior of traffic flow as manifested by the distinction in the character of traffic flow in the uncongested and congested regimes, and particularly as a consequence of the discontinuity in volume. His observations generally accord with the views of many freeway operations traffic engineers who recognize the instability of traffic near peak volumes. The general principle that is derived from this understanding is a need to operate the freeways at volumes less than peak volumes to avoid a transition to the congested regime with an associated substantial reduction in volume.

A full understanding of the discontinuity is not yet available. One expects that the basis for the discontinuity should be traceable to specific characteristics of driver-vehicle behavior. Some suggestions along these lines were presented by Ceder (5), but no definitive studies have been done. Recently, however, Cohen, according to a private communication, has made controlled simulation runs using the microscopic INTRAS model (18,19), which have also

TABLE 3 Summary of Regression Results

	FULL CALIBRATION										CALIBRATION TO STANDARD FORM		
				IMPEDED REGIME			CONSTRAINED REGIME						
DATA SET	CAPACITY VEH/LN-HR	FREE SPEED MI/HR	FIRST BREAKPOINT VEH/LN-MI	u_1 MI/HR	α	SECOND BREAKPOINT VEH/LN-MI	OFFSET MI/HR	β_0	β_1	FIT MI/HR	*** SCALE FACTOR	CAPACITY* VEH/LN-HR	*** FIT MI/HR
SME12	2177	55.1	20	63.8	-.423	52	28	$.867\times10^{-2}$	$.139\times10^{-3}$	1.90	1.0706	2287	2.55
SME18	2069	51.4	20	57.8	-.328	50	28	$.903\times10^{-2}$	$.153\times10^{-3}$	1.95	.9962	2128	2.14
HAS13	2096	49.0	27	57.4	-.310	50	NO DATA AVAILABLE			1.53	1.0163	2171	1.54
HAS18	2147	50.0	12	53.5	-.295	60	28	$.975\times10^{-2}$	$.135\times10^{-3}$	1.17	.9457	2020	1.81
HAS24	2237	47.0	33	56.3	-.284	55	28	$.700\times10^{-2}$	$.167\times10^{-3}$	1.76	1.0245	2188	1.56
COMPOSITE	2136*	58.1	0	58.1	-.351	50/60**	28	$.912\times10^{-2}$	$.141\times10^{-3}$	2.68			

*Extrapolated to volume at density of 55 veh/ln-mi.

**Data with densities in the range 50-60 veh/ln-mi were excluded from the regression analysis.

***Root-mean-squared-error.

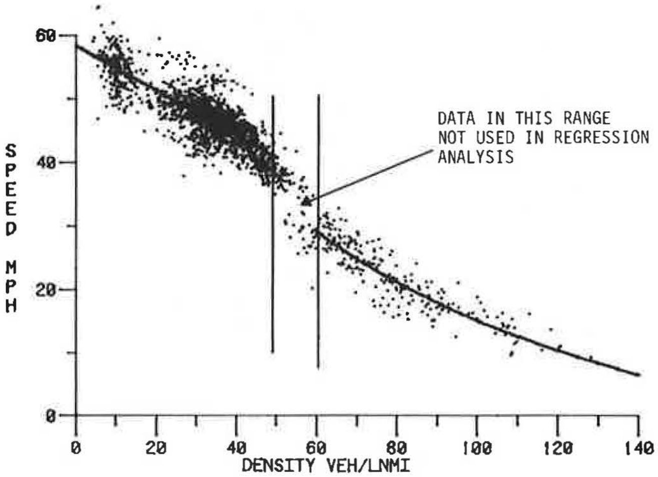

FIGURE 6 Regression for composite data set (speed-density).

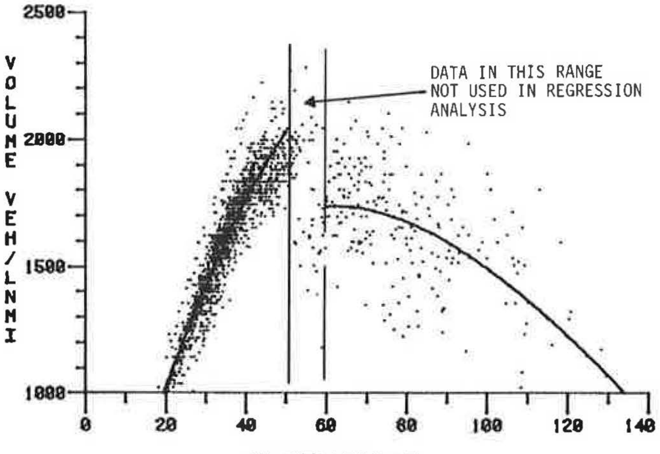

FIGURE 7 Regression for composite data set (volume-density).

exhibited a reduction of substantial volume after breakdown in a lane-drop situation (INTRAS models individual car behavior).

Figure 8 shows such a lane-drop situation with associated ramps. Uncontrolled, traffic can enter the upstream on-ramp in such volume as to exceed the capacity, leading to breakdown (i.e., transition to the congested conditions). In a long section of two

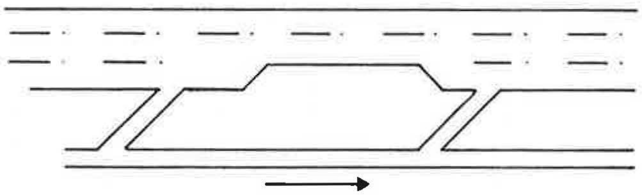

FIGURE 8 Freeway bottleneck.

lanes, the capacity will as a result be substantially reduced, contributing further to congestion and delay. On-ramp control, either by storing vehicles at the ramp or by diverting vehicles to an alternate route, can prevent breakdown and thereby maintain a higher service rate (i.e., volume along the two-lane section).

Traffic dynamics are substantially more complex than this simple analysis might suggest. The FREFLO model, by representing effects due to spatial variations in density, for example, admits increased volumes above the congested capacity in transition areas (e.g., at the head of a queue). This effect is also observed in real traffic. As a result, the effect of the discontinuity can be overcome in small areas. Development of control strategies to account for the discontinuity in volume must therefore be fairly sophisticated and take into account dynamic as well as the underlying static equilibrium relationships.

ACKNOWLEDGMENT

This research was conducted under Contract DTFH61-81-C-00038, sponsored by the Federal Highway Administration, Steven Cohen and Paul Ross, contract managers.

REFERENCES

1. L.C. Edie. Car-following and Steady State Theory for Noncongested Traffic. Operations Research, Vol. 9, No. 1, 1961, pp. 66-76.
2. P. Athol. Interdependence of Certain Operational Characteristics Within a Moving Traffic Stream. In Highway Research Record 72, HRB, National Research Council, Washington, D.C., 1965, pp. 58-87.
3. J.S. Drake, J.L. Schoefer, and A.D. May, Jr. A Statistical Analysis of Speed Density Hypotheses. In Highway Research Record 154, HRB,

National Research Council, Washington, D.C., 1967, pp. 53-87.

4. A.D. May, Jr. and H.E.M. Keller. Evaluation of Single- and Two-Regime Traffic Flow Models. Proc., 4th International Symposium on the Theory of Traffic Flow, Karlsruhe, 1968.
5. A. Ceder. Investigation of Two-Regime Traffic Flow Models at the Micro- and Macroscopic Levels. Ph.D. dissertation. University of California, Berkeley, 1975.
6. H.S. Mika, J.B. Kreer, and L.S. Yuan. Dual-Mode Behavior of Freeway Traffic. In Highway Research Record 279, HRB, National Research Council, Washington, D.C., 1969, pp. 1-12.
7. H.J. Payne. Models of Freeway Traffic and Control. Mathematics of Public Systems, Vol. 1, 1971, pp. 51-61.
8. E. Lieberman, B. Andrews, M. Davila, and M. Yedlin. Macroscopic Simulation for Urban Traffic Management, 3 volumes. Report FHWA-RD-80-113, 114, and 115. Office of Research and Development, FHWA, U.S. Department of Transportation, 1982.
9. A.G.R. Bullen. Strategies for Practical Expressway Control. Proc., ASCE 1972 and Transportation Engineering Journal, Aug. 1972.
10. P. Athol and A.G.R. Bullen. Multiple Ramp Control for a freeway Bottleneck. In Highway Research Record 456, HRB, National Research Council, Washington, D.C., 1973, pp. 50-54.
11. D.C. Haughton. A Mackov Model for Expressway Control. Presented at Operation Research Society of America National Meeting, Las Vegas, Nevada, 1975.
12. H.J. Payne and C. Wolfe. Macroscopic Simulation for Urban Traffic Management, The TRAFLO Model, General Technical Specifications, Supplement: Macroscopic Freeway Model. Report ES-R-B001-2. ESSCOR, San Diego, Calif., Oct. 1978.
13. H.J. Payne. FREFLO: A Macroscopic Simulation Model of Freeway Traffic (Version I), User's Guide. ESSCOR Report ES-R-78-1. July 1978.
14. H.J. Payne. A Critical Review of a Macroscopic Freeway Model. In Computer Control of Urban Traffic Systems, Pacific Grove, Calif., 1979, pp. 251-265.
15. H.J. Payne. Calibration and Validation of FREFLO, Vol. I: User Calibration Procedures and Supporting Data Analysis. VERAC Report R-001-82. VERAC, Inc.; FHWA, U.S. Department of Transportation, Dec. 1981.
16. H.J. Payne and E.D. Helfenbein. Freeway Surveillance Data. Report FHWA-RD-76-74. FHWA, U.S. Department of Transportation, April 1976.
17. Data tapes PD 263 644/AS and PD 263 543/AS. National Technical Information Service.
18. D.A. Wicks and E.B. Lieberman. Development and Testing of INTRAS, a Microscopic Freeway Simulation Model, Vol. 1: Program Design and Parameter Calibration. Report KLD TR-40. KLD Associates; FHWA, U.S. Department of Transportation, Jan. 1976.
19. D.A. Wicks and B.J. Andrews. Development and Testing of INTRAS, a Microscopic Freeway Simulation Model, Vol. 2: User's Manual. Report FHWA-RD-076-77. FHWA, U.S. Department of Transportation, June 1977.

Publication of this paper sponsored by Committee on Traffic Flow Theory and Characteristics.